Randomized Pulse Pattern Strategy of Synchronized SVPWM for Low-Frequency-Ratio Applications

Kun He, *Member, IEEE*, Jian Li, *Senior Member, IEEE*, Lifan Xiao, *Member, IEEE*, Yongqian Xiong, and Linghao Wu

***Abstract*—Low switching frequency operation is preferred in machine drives of high-power applications for controlling the switching loss of power-electronic devices to a tolerable level. Hence, the modulation frequency ratio is usually low. Synchronized space vector pulsewidth modulation (synchronized SVPWM) is a method designed to reduce current harmonic distortion in low-frequency-ratio occasions. However, the switching frequency apparently varies when the pulse pattern of synchronized SVPWM changes, which makes it impossible to fully use the available switching frequency. In this article, the alternative pulse patterns of synchronized SVPWM are extended by the proposed randomized pulse pattern strategy. The proposed strategy divides pulse patterns in a line cycle of the synchronized SVPWM into six pulse pattern units according to the symmetry conditions, and randomly combines these pulse pattern units according to the probability theory. The pulse pattern units from different pulse patterns are analyzed and modified to concatenate together smoothly. The proposed strategy keeps the advantages of synchronized SVPWM that low-order harmonics are suppressed. Meanwhile, lower harmonic distortion and torque ripples are achieved compared with the conventional strategy. The proposed strategy is verified through simulations and experiments.**

***Index Terms*—High-power drives, low frequency ratio, machine control, randomized pulsewidth modulation (PWM), synchronized PWM.**

I. Introduction

LOW switching frequency operation is frequently adopted in machine drives of high-power applications like high-speed railways to control the switching loss of power-electronic devices to an acceptable level [1]–[6]. Under low switching frequency conditions, the high fundamental frequency will make the frequency ratio of the modulation very low. Conventional modulation methods like space vector pulsewidth modulation (SVPWM) show poor performance in such cases. For example, the total harmonic distortion (THD) will be high and low-order harmonics will be unacceptable. Researchers have proposed kinds of modulation methods to improve the performance in low-frequency-ratio operation. Synchronized SVPWM [7]–[9], optimal PWM [10]–[12], and specified-harmonic-elimination PWM (SHE-PWM) [13], [14] are three popular modulation methods. Among these methods, synchronized SVPWM is attractive due to the balance between the implementation complexity and the performance in harmonic distortion. Like all other synchronized modulation methods, synchronized SVPWM circumvent the low-order harmonics, and subharmonics [15].

Since synchronized SVPWM was proposed, a number of researchers have reported improvements on this method [16]–[21]. Wang, *et al.* [16] applied synchronized SVPWM in the drive of six-phase machine. Beig [20] discussed the overmodulation strategy of synchronized SVPWM in a three-level inverter. Diao *et al.* [17] proposed an efficient implementation of hybrid PWM, which includes synchronized SVPWM in. However, despite these works, a problem of synchronized SVPWM still remains to be solved. Synchronized SVPWM has fixed pulse patterns, which means the switching frequency can only be fixed integer multiples of the fundamental frequency. When fundamental frequency increases, the employed pulse pattern must change to make sure the switching frequency does not exceed the limit. Therefore, the available switching frequency cannot be fully utilized in almost all the fundamental frequency ranges. The drop in switching frequency may lead to problems like performance degradation in current control and an apparent increase of current harmonics. Besides, the discontinuous in pulse numbers brings inconvenience in the application in which the switching frequency needs to be dynamically adjusted.

Researchers have tried to solve this problem by adding more available pulse patterns [7]. By using proper bus-clamping strategies, pulse patterns with pulse number 3, 5, 7, . . . , 15 can be achieved. A denser pulse pattern list moderates the variation in switching frequency, but the results are still not completely satisfactory. The first problem is that some pulse patterns with high pulse number do not have corresponding more excellent harmonic performance. For instance, the pulse pattern with pulse number seven generates higher harmonics than pulse patterns with pulse number five due to its excess restrictions on the implementation method [22]. The second problem is that the

Manuscript received June 19, 2020; revised September 23, 2020; accepted October 27, 2020. Date of publication November 2, 2020; date of current version February 5, 2021. This work was supported by the National Natural Science Foundation of China under Grant 51877094. Recommended for publication by Associate Editor A. M. Trzynadlowski. *(Corresponding author: Jian Li.)*

Kun He, Jian Li, Lifan Xiao, and Yongqian Xiong are with the State Key Laboratory of Advanced Electromagnetic Engineering and Technology, School of Electrical and Electronic Engineering, Huazhong University of Science and Technology, Wuhan 430074, China (e-mail: kun_he@hust.edu.cn; jianli@hust.edu.cn; lifanxiao@hust.edu.cn; yqxiong@hust.edu.cn).

Linghao Wu is with the Engineering Research Center of Novel Electrical Machines and Special Electromagnetic Equipments, Ministry of Education, Beijing 100816, China (e-mail: 2604957535@qq.com).

Color versions of one or more of the figures in this article are available online at https://ieeexplore.ieee.org.

Digital Object Identifier 10.1109/TPEL.2020.3035199

switching frequency still drops at least 40% when applying the pulse pattern with pulse number three.

In this article, the authors try to solve this problem from another perspective. This article is contributed to using probability theory to generate pulse patterns with fractional pulse numbers, and generating little extra harmonics at the same time. Random PWM has been researched mainly for reducing EMI of inverters [23]–[25]. The essential idea of random PWM is using a random-frequency modulation carrier. However, the conventional random PWM cannot be applied in low-frequency-ratio operations because it will destroy the synchronization and deteriorate low-order harmonic performance. In low-frequency-ratio applications, the synchronization must be maintained with a random frequency carrier. In order to achieve this target, the conventional pulse patterns of synchronized SVPWM in a fundamental period are divided into six pulse pattern units according to the symmetrical conditions, and proper modification is made to pulse pattern units so that the units from different pulse patterns can be arbitrarily combined. The randomized selecting strategy of pulse pattern units are proposed based on probability theory to guarantee the average switching frequency at the target value. By means of the proposed randomized pulse pattern strategy, the fast Fourier transform (FFT) spectrum of current and torque become more dispersed and have a considerable reduction in primary harmonic orders, which is beneficial to reduce the noise-vibration-harshness of machines as many researchers proved [26], [27].

The rest of this article is organized as follows. Section II introduces the pulse patterns of the synchronized SVPWM. Section III elaborates on the proposed randomized pulse pattern strategy. In this section, the idea of the pulse pattern unit is firstly introduced. Then, the pulse pattern units from different pulse patterns are analyzed and modified to be smoothly combined with each other. Finally, the selecting strategy of pulse pattern units is demonstrated. In Section IV, simulations and experiments verify the effectiveness of the proposed strategy. Finally, Section V concludes the article.

II. Synchronized SVPWM

A. Pulse Patterns of Synchronized SVPWM

Synchronized SVPWM is a common modulation method in low-frequency-ratio applications for reducing harmonic distortions. In synchronized SVPWM, pulse patterns with different pulse numbers are applied in different frequency-ratio cases, which are implemented with half-wave symmetry (HWS), quad-wave symmetry (QWS), and three-phase symmetry (TPS) conditions. For a pulse pattern, the pulse number is represented by $\boldsymbol{P}$, and the frequency ratio is represented by $\boldsymbol{N}$

$$\boldsymbol{P} = \frac{f_{\mathrm{sw}}}{f_e},\ \boldsymbol{N} = \frac{f_s}{2f_e}. \tag{1}$$

In (1), f_e is the machine fundamental frequency, f_{sw} is the switching frequency, and f_s is the sampling frequency. The existence of coefficient 2 in the calculation of $\boldsymbol{N}$ is because of the asymmetric sampling. For convenience, the pulse pattern with pulse number x is written as $\boldsymbol{P}_x$ in this article. Because high-frequency-ratio synchronized SVPWM has no significant advantage over asynchronous SVPWM, only pulse patterns whose pulse numbers do not exceed 15 are discussed in this article. The available basic pulse patterns of synchronized SVPWM are listed in Table I. In the table, the numbers in the vector sequence column represent how a space vector is modulated by six active vectors and two zero vectors. For example, 0127 mean a vector is modulated in the sequence $V_0V_1V_2V_7$. Some of the basic pulse patterns can be realized by different vector sequences marked I and II. Proper bus-clamping strategy helps achieve more pulse patterns. The pulse patterns with bus-clamping strategy is listed in Table II. Additionally, proper vector position and modulation vector sequence further extend the alternative pulse patterns, as shown in Table III. Some pulse patterns are not shown in these tables due to their complex implementations and unsatisfactory harmonic performance. All the three kinds of implementations are detailed in [22] and a full list of pulse patterns in synchronized SVPWM can be found in [7].

TABLE I
Basic Pulse Patterns

$\boldsymbol{P}$	$\boldsymbol{N}$	Vector Position in Sector I	Vector Sequence
15	15	6°, 18°, 30°, 42°, 54°	I: 0127, 7210, 0127, 7210, 0127
			II: 7210, 0127, 7210, 0127, 7210
9	9	10°, 30°, 50°	I: 0127, 7210, 0127
			II: 7210, 0127, 7210
3	3	30°	0127

TABLE II
Bus-Clamped Pulse Patterns

$\boldsymbol{P}$	$\boldsymbol{N}$	Vector Position in Sector I	Vector Sequence
11	15	6°, 18°, 30°, 42°, 54°	012, 210, 0127, 721, 127
7	9	10°, 30°, 50°	127, 7210, 012

TABLE III
Special Vector Sequence Pulse Patterns

$\boldsymbol{P}$	$\boldsymbol{N}$	Vector Position in Sector I	Vector Sequence
13	18	0°, 10°, 20°, 30°, 40°, 50°, 60°	010, 012, 210, 0127, 721, 127, 727
5	6	0°, 30°, 60°	010, 0127, 727

B. Steady-State Flux Trajectory of Pulse Patterns

When the stator resistance of a machine is ignored, the integration of voltage vectors in a pulse pattern can be regarded as the steady-state stator flux. The flux trajectory is depicted according to the basic active voltage vectors of the vector sequences, as in Tables I–III. Every pulse pattern has a corresponding stator flux trajectory. The flux trajectories of $\boldsymbol{P}_5$ and $\boldsymbol{P}_9$ are demonstrated in Fig. 1. As shown in Table I, pulse patterns $\boldsymbol{P}_{15}$ and $\boldsymbol{P}_9$ have

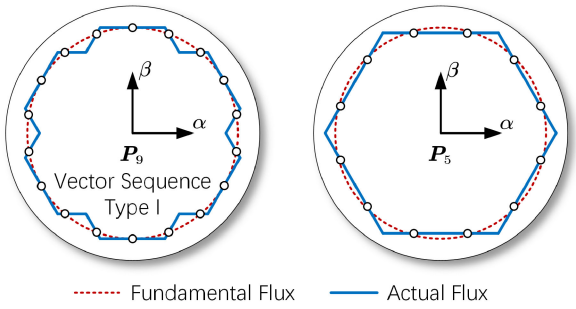

Fig. 1. Flux trajectories of $\boldsymbol{P}_9$ and $\boldsymbol{P}_5$.

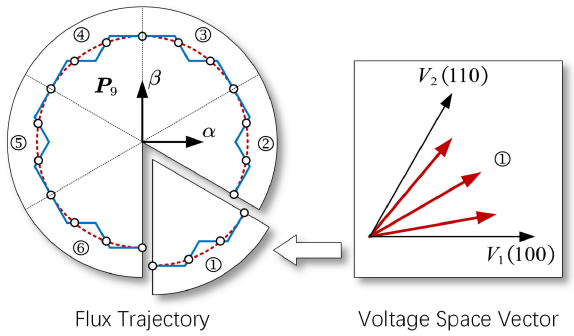

Fig. 2. Unit of $\boldsymbol{P}_9$. The voltage vectors in a pulse pattern unit and the corresponding flux trajectory are depicted.

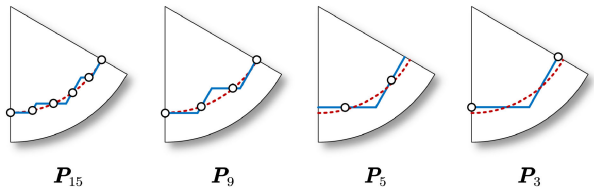

Fig. 3. Pulse pattern units represented in the form of flux trajectory.

two vector sequence types corresponding to two different kinds of flux trajectorys. However, the harmonic performance of type I and II are similar. Hence, only type I is discussed and employed in this article. The circles on the flux trajectory are the points when modulation periods end. The flux trajectory is a vital characteristic of a pulse pattern and the proposed randomized pulse pattern strategy is constructed based on that.

III. Strategy of Pulse Pattern Randomization

In synchronized SVPWM, a specific pulse pattern is selected for a particular fundamental frequency. However, in most cases, the available switching frequency cannot be fully utilized because there is no corresponding pulse pattern. Conventionally, the pulse pattern whose switching frequency will not exceed the limits is adopted. Nevertheless, when pulse number is low, the change of pulse pattern brings a dramatic change in switching frequency. For example, when pulse pattern changes from $\boldsymbol{P}_5$ to $\boldsymbol{P}_3$, the switching frequency drops 40%, which leads to an apparent increase in harmonics. In this article, this problem is solved by the randomized pulse pattern strategy. Two pulse patterns are randomly applied so that the available switching frequency can be fully utilized.

A. Pulse Pattern Unit

The purpose of the proposed randomized pulse pattern strategy is to apply different pulse patterns randomly to achieve the target average switching frequency based on probability theory. In order to achieve randomization, a complete pulse pattern in a single fundamental period is first divided into six pulse pattern units. According to the symmetry condition of synchronized SVPWM, the voltage space vectors in a sector is the minimal representation of a pulse pattern. The flux trajectory has a periodicity of 60°. Hence, it is appropriate to select the vectors in a sector as the unit of pulse pattern and which is the smallest operable unit. The flux trajectory unit of $\boldsymbol{P}_9$ and its corresponding voltage vectors in unit 1 are shown in Fig. 2. Therefore, it exists six instance to switch pulse pattern units in a fundamental period.

The flux trajectories of pulse pattern units in $\boldsymbol{P}_3, \boldsymbol{P}_5, \boldsymbol{P}_9, \boldsymbol{P}_{15}$ are shown in Fig. 3. These pulse patterns are selected for the randomized pulse pattern strategy according to the harmonics performance and implementation complexity. The purpose of the proposed strategy is to generate randomized pulse patterns whose pulse number is between pulse numbers of the adjacent conventional pulse patterns. Hence, it is unnecessary to select too many conventional pulse patterns.

B. Combination of Pulse Pattern Units

The randomization of pulse patterns requires to combine different pulse pattern units in a single fundamental period. The combination is permitted only at the boundary of pulse pattern unit. Generally, only two pulse patterns with adjacent pulse number will be applied in a specific working point. However, not all units in different pulse patterns can be directly combined. Two questions need to be concerned in the combination process:

1) whether the combination of two pulse pattern units causes extra switching events;
2) whether the flux continuity of two pulse pattern units are kept without generating any extra harmonics when combination is conducted.

The phase leg states, $S_aS_bS_c$, at the beginning of the pulse pattern units, decides the number extra switching events in combining different pulse pattern units. $S_{a/b/c} = 1$ means the upper phase leg is on and the lower phase leg is off. $S_{a/b/c} = 0$ means the upper phase leg is off and the lower phase leg is on. Only the initial phase leg states of pulse pattern units indexed 1 and 2 need to be concerned, and the $S_aS_bS_c$ of other 4 units can be deduced via them according to the symmetry conditions. The $S_aS_bS_c$ of different pulse patterns in unit 1 and unit 2 depends on the starting and ending basic voltage vectors, and which are related to their implementation methods, as shown in Tables I and III. For basic pulse patterns in Table I, all vector sequence starts with V_0 and ends with V_7 with type I implementation method considered only. However, the pulse

TABLE IV
INITIAL PHASE LEG STATES OF PULSE PATTERN UNITS

	$S_aS_bS_c$ in Unit 1	$S_aS_bS_c$ in Unit 2
$\boldsymbol{P}_3$	000	111
$\boldsymbol{P}_5$	100	110
$\boldsymbol{P}_9$	000	111
$\boldsymbol{P}_{15}$	000	111

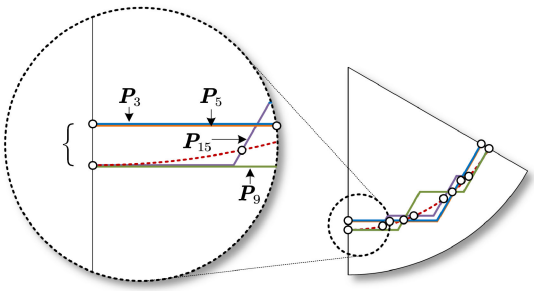

Fig. 4. Zoomed-in view of the differences between fundamental flux and actual flux at the start of the pulse pattern unit.

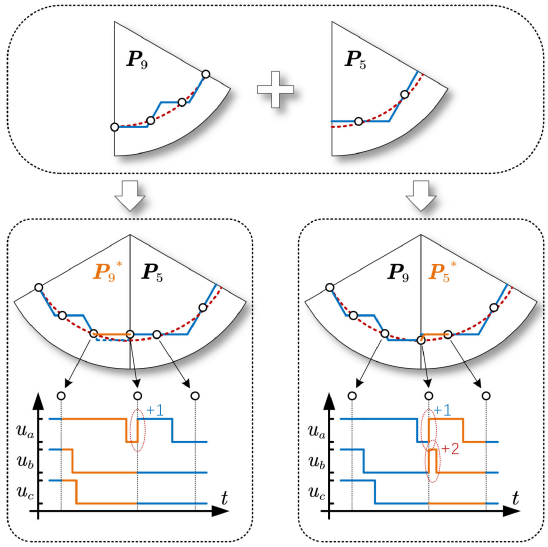

Fig. 5. Modification of pulse pattern unit in the randomization between $\boldsymbol{P_9}$ and $\boldsymbol{P_5}$. The modification on different pulse pattern units will lead to different number of extra switches.

pattern $\boldsymbol{P}_5$ is implemented with boundary vectors at 0° and 60°, so its basic voltage vectors at the boundary of Sector I are V_1 and V_2, respectively. In Table IV, the initial phase leg states of all the selected pulse patterns are summarized, which plays a vital role in pulse pattern units combination process. From the table, it can be found that the combination of pulse pattern units from $\boldsymbol{P}_5$ and units from other pulse pattern will lead to one extra switching event.

The answer to the second question is similar to the pulse pattern transition strategy in the conventional synchronized SVPWM strategy [18], [22]. However, in the randomized pulse pattern synchronized SVPWM, the combination needs to be more carefully considered because the pulse pattern will change in a much higher frequency. For the purpose of avoiding extra harmonics and oscillations, the combined two pulse pattern units must have the same modulation index. Besides, the magnitude of the actual stator flux at the connecting point must be the same. In the cases where the two conditions are satisfied, the actual stator flux trajectory will be connected smoothly between flux trajectories of the two pulse pattern units, and the steady state can be maintained. The consistency of modulation indexes in different modulation units can be easily guaranteed. However, it can be found in Fig. 3 that the boundary flux magnitude of the same-MI pulse pattern units may be different. The relationship between boundary actual flux magnitude and fundamental flux magnitude of the selected pulse pattern units are illustrated in Fig. 4 and evaluated quantitatively in (6). The difference mainly exists between the pulse pattern units from $\boldsymbol{P}_5$ and $\boldsymbol{P}_9$. Hence, an additional adjustment should be applied.

A natural idea to eliminate the differences in flux magnitude is to adjust the flux trajectory of a pulse pattern to match the start point of the pulse pattern unit with others. This adjustment works on the voltage space vectors of pulse pattern units.

TABLE V
EXTRA SWITCHING EVENTS IN PULSE PATTERN UNIT COMBINATION

$\boldsymbol{P}_x$	$\boldsymbol{P}_y$	Combination	Modifing $\boldsymbol{P}_x$	Modifing $\boldsymbol{P}_y$
3	5	+1	-	-
5	3	+1	-	-
5	9	+1	+2	+0
9	5	+1	+0	+2
9	15	+0	-	-
15	9	+0	-	-

Assuming that $\boldsymbol{P}_x$ will be combined with $\boldsymbol{P}_y$, the adjustment can take place in either the units of $\boldsymbol{P}_x$ or the units of $\boldsymbol{P}_y$. The modification in different pulse pattern units will lead to different extra switching events. The combination of pulse pattern units of $\boldsymbol{P}_5$ and $\boldsymbol{P}_9$ is shown in Fig. 5. When the unit of $\boldsymbol{P}_5$ is adjusted, two extra switching events appear. When the unit of $\boldsymbol{P}_9$ is adjusted, there is no extra switching event. Table V shows the number of extra switching events in pulse pattern unit combination. From the table, it can be found that the pulse pattern unit of $\boldsymbol{P}_9$ is preferred to be modified in the randomization between $\boldsymbol{P}_5$ and $\boldsymbol{P}_9$.

For analyzing how to adjust the pulse pattern unit, the modulation indexes of pulse patterns should be first clarified. Under low-frequency-ratio conditions, the relationship between the modulation index and modulation vector length becomes more complicated than in high-frequency-ratio cases. By defining the modulation vector length as m and the modulation index as MI as (2), where U_1 is the fundamental voltage magnitude, U_s is reference voltage vector magnitude. The complex relationship can be revealed through Fourier analysis. The relationship of m and MI can be expressed as (3)

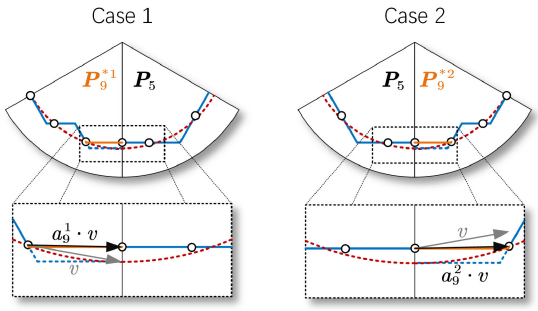

Fig. 6. Modification factor on vectors in the randomization between $\boldsymbol{P}_5$ and $\boldsymbol{P}_9$.

$$\text{MI} = \frac{U_1}{V_{\text{dc}}/2}, \quad m = \frac{U_s}{2V_{\text{dc}}/3} \tag{2}$$

$$\text{MI} = \begin{cases} 1.47\,m, & \boldsymbol{P}_3 \\ 1.37\,m, & \boldsymbol{P}_5 \\ 1.33\,m, & \boldsymbol{P}_9 \text{ and } \boldsymbol{P}_{15}. \end{cases} \tag{3}$$

The difference between the actual flux magnitude $|\boldsymbol{\psi}_{\text{act}}|$, and the fundamental flux magnitude $|\boldsymbol{\psi}_{\text{fund}}|$, at the beginning of a pulse pattern unit can be calculated according to (3). For a pulse pattern, $|\boldsymbol{\psi}_{\text{act}}|$ can be calculated as

$$|\boldsymbol{\psi}_{\text{fund}}| = \frac{1}{2\omega_e}\text{MI} \cdot V_{\text{dc}} \tag{4}$$

where ω_e is the angular electric frequency and V_{dc} is the dc bus voltage. Meanwhile, according to symmetry, the starting point of the flux, the ending point of the flux, and the origin construct a equilateral triangle. Hence, $|\boldsymbol{\psi}_{\text{act}}|$ can be calculated by integrating the voltage space vector in the pulse pattern unit. For example, $|\boldsymbol{\psi}_{\text{act}}|$ of units in $\boldsymbol{P}_9$ is

$$|\boldsymbol{\psi}_{\text{act}}| = \frac{4\pi V_{\text{dc}}}{3\omega_e}|me^{\text{j}\frac{\pi}{18}} + me^{\text{j}\frac{\pi}{6}} + me^{\text{j}\frac{5\pi}{18}}|. \tag{5}$$

With $|\boldsymbol{\psi}_{\text{act}}|$ and $|\boldsymbol{\psi}_{\text{fund}}|$, the differences can be found, which are

$$k_\psi = \frac{|\boldsymbol{\psi}_{\text{act}}|}{|\boldsymbol{\psi}_{\text{fund}}|} = \begin{cases} 0.95, & \boldsymbol{P}_3 \\ 0.95, & \boldsymbol{P}_5 \\ 1.00, & \boldsymbol{P}_9 \text{ and } \boldsymbol{P}_{15}. \end{cases} \tag{6}$$

From the equation, the modification on the pulse pattern unit can be constructed. The modification works on the vector next to a different pulse pattern unit. In the randomization of $\boldsymbol{P}_5$ and $\boldsymbol{P}_9$, two modification cases exist, which are shown in Fig. 6. The vector adjustment factors of these two cases can be calculated by k_ψ and the sampling frequency f_s of the two patterns, which are

$$a_9^1 = 0.985\text{e}^{\text{j}9.21^\circ}, \; a_9^2 = 0.985\text{e}^{-\text{j}9.21^\circ}. \tag{7}$$

The modification on the pulse pattern unit guarantees the continuity of the flux trajectory in the randomization, which ensures that the machine will be in steady state after a new pulse pattern unit is employed. However, the modification inevitability affects the fundamental flux magnitude. This phenomenon is only obvious in the randomization between $\boldsymbol{P}_9$ and $\boldsymbol{P}_5$. The effect is demonstrated by the pulse pattern unit sequence $\boldsymbol{P}_9^*\boldsymbol{P}_5\boldsymbol{P}_9^*\boldsymbol{P}_5\boldsymbol{P}_9^*\boldsymbol{P}_5$. The corresponding flux trajectory is shown in Fig. 7, where the modified flux trajectory is denoted as yellow solid line, which only occurred in pulse pattern $\boldsymbol{P}_9$ due to fewer extra switching events as aforementioned. The harmonic performance of the modulation is evaluated by dc-normalized weighted harmonic distortion (WTHD0). The pulse pattern sequence can be regarded as the worst case because the modification are as much as possible. In this case, when required modulation index $\text{MI}^* = 0.8$, the actual modulation index $\text{MI} = 0.79$, and the WTHD0 is 4.39%. The modulation index of the randomized pulse pattern slightly deviate from the reference. Comparing with the original pulse pattern $\boldsymbol{P}_9$ whose WTHD0 is 4.04% and $\boldsymbol{P}_5$ whose WTHD0 is 5.26%, the WHTD0 of the randomized pulse pattern 4.39% is slightly different from the average WTHD0 of the two pulse patterns, which is 4.65%. The negative effect is acceptable, considering the benefit of the randomization.

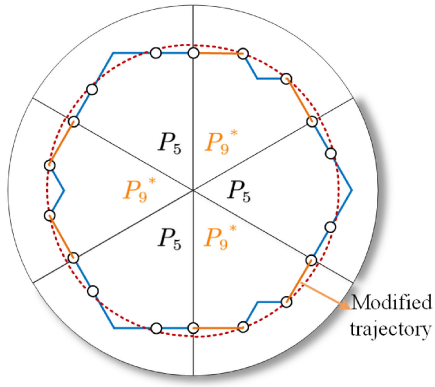

Fig. 7. Flux trajectory of pulse pattern sequence $\boldsymbol{P}_9^*\boldsymbol{P}_5\boldsymbol{P}_9^*\boldsymbol{P}_5\boldsymbol{P}_9^*\boldsymbol{P}_5$.

C. Randomized Selection of Pulse Pattern Units

The strategy discussed in the previous section lead to minimal negative impact when the two pulse pattern units are combined. A remaining question is how to select pulse pattern units in a fundamental period. In this part, the authors developed an algorithm for pulse pattern selection based on the expectation of the switching frequency.

Assuming the desired switching frequency is f_{sw}, the randomization method should make the actual switching frequency f_{act}, equal to f_{sw}. This objective is realized by considering the expectation of switching frequency when randomly selecting pulse pattern units. In the implementation of the modulation strategy, a sequence is maintained, which contains the following three pulse pattern units for modulation. When the reference voltage enters a new sector, the first pulse pattern unit in the sequence, which takes effect is removed, while a new pulse pattern unit is added to the sequence. The process is shown in Fig. 8. The new pulse pattern unit is selected by a random method. The steps of selecting the new pulse pattern unit are expressed as follows.

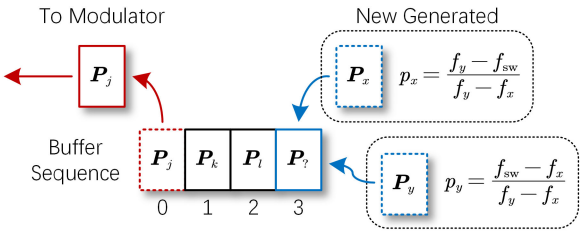

Fig. 8. Sequence of pulse pattern unit for modulation.

1) Select pulse patterns $\boldsymbol{P}_x$ and $\boldsymbol{P}_y$ for randomization strategy. The selected pulse pattern should satisfy

$$xf_e < f_{\text{sw}} < yf_e. \tag{8}$$

2) Verify the previous pulse pattern $\boldsymbol{P}_l$ and the numbers of extra switches n_x, n_y when connecting $\boldsymbol{P}_x$ and $\boldsymbol{P}_y$ with $\boldsymbol{P}_l$. Calculate the switching frequency when using $\boldsymbol{P}_x$ and $\boldsymbol{P}_y$

$$f_x = (x + n_x)f_e,\ f_y = (y + n_y)f_e. \tag{9}$$

3) Calculate the probabilities of selecting $\boldsymbol{P}_x$ and $\boldsymbol{P}_y$, which makes the expectation of switching frequency equal f_{sw}

$$p_x = \frac{f_y - f_{\text{sw}}}{f_y - f_x},\ p_y = \frac{f_{\text{sw}} - f_x}{f_y - f_x}. \tag{10}$$

4) Generate a random number r, in range $[0, 1]$. If $r \le p_x$, select $\boldsymbol{P}_x$. Else, select $\boldsymbol{P}_y$.

The strategy ensures the switching frequency expectation of the selected pulse pattern unit matches f_{sw}, as

$$E(f_{\text{act}}) = p_x f_x + p_y f_y = f_{\text{sw}} \tag{11}$$

which means a pulse pattern $\boldsymbol{P}_{f_{\text{sw}}/f_e}$ is generated by randomization. Theoretically, any pulse pattern between $\boldsymbol{P}_x$ and $\boldsymbol{P}_y$ can be realized by the randomization method. However, if the probability of selecting a pulse pattern unit is too low, the pulse pattern unit may be selected only once in a couple of fundamental periods. Hence, the lowest proportion of a pulse pattern is limited to $1/6$, which avoids the harmonics lower than the fundamental frequency. Within the limit, the available pulse patterns are

$$\boldsymbol{P}'_{3.67-5}, \boldsymbol{P}'_{6-8.67}, \boldsymbol{P}'_{10-14}, \tag{12}$$

where the superscript $'$ means the pulse pattern is generated by randomization.

D. Switching Frequency Compensation

When selecting the pulse pattern unit, a negative probability may appear in (10) because of the switching frequency correction in (9). If the negative probability is limited to zero, an error in $E(f_{\text{act}})$ will appear and result in an error in average switching frequency, an example of which is realizing $\boldsymbol{P}'_{3.8}$ by randomization between $\boldsymbol{P}_3$ and $\boldsymbol{P}_5$. When the previous pulse pattern unit belongs to $\boldsymbol{P}_5$, selecting $\boldsymbol{P}_3$ as $\boldsymbol{P}_x$ will lead to negative p_x in (10). If p_x is set to zero, $E(f_{\text{act}})$ will be $4f_e$, which is higher than the desired switching frequency $3.8f_e$. Hence, a switching frequency compensation is introduced. The

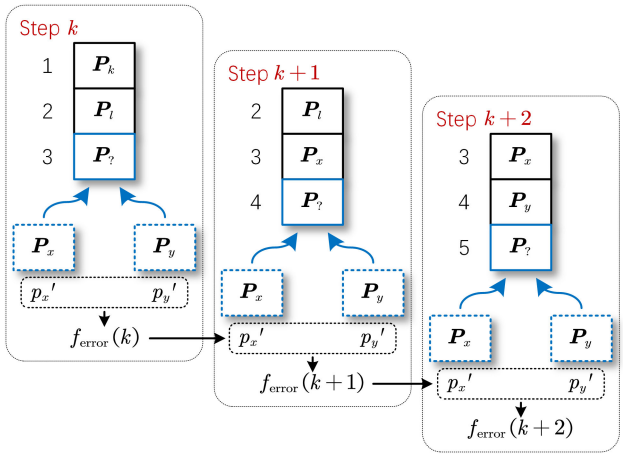

Fig. 9. Switching frequency compensation in probability calculation of pulse pattern unit selection.

compensated process of pulse pattern unit selection is shown in Fig. 9. When the $E(f_{\text{act}})$ does not equal f_{sw}, the error will be recorded and affect the following process. The average of $E(f_{\text{sw}})$ in times of pulse pattern selection selection will equal f_{sw}. The steps of pulse pattern unit selection with switching frequency compensation is expressed as follows.

1) When the available pulse pattern P_{f_{sw}/f_e}, is in (12), select $\boldsymbol{P}_x$ and $\boldsymbol{P}_y$ for randomization strategy. $\boldsymbol{P}_x$ and $\boldsymbol{P}_y$ should satisfy (8).
2) Verify the previous pulse pattern $\boldsymbol{P}_l$ and the numbers of extra switches n_x and n_y, when connecting $\boldsymbol{P}_x$ and $\boldsymbol{P}_y$ with $\boldsymbol{P}_l$. Calculate the corresponding switching frequency using (9).
3) Calculate the desired switching frequency in this round of pulse pattern unit selection as

$$f'_{\text{sw}} = f_{\text{sw}} - f_{\text{error}}(k-1) \tag{13}$$

in which $f_{\text{error}}(k-1)$ is the switching frequency error in the last round of pulse pattern unit selection.
4) Calculate the probability p_x and p_y of selecting $\boldsymbol{P}_x$ and $\boldsymbol{P}_y$

$$p_x = \frac{f_y - f'_{\text{sw}}}{f_y - f_x},\ p_y = \frac{f'_{\text{sw}} - f_x}{f_y - f_x}. \tag{14}$$

5) Limit p_x and p_y to range $[1/6, 5/6]$, the limited probabilities are p'_x and p'_y.
6) Generate a random number r in range $[0, 1]$. If $r < p'_x$, select $\boldsymbol{P}_x$, else select $\boldsymbol{P}_y$.
7) Calculate the expectation of actual switching frequency using

$$E(f_{\text{act}}) = p'_x f_x + p'_y f_y \tag{15}$$

and update the switching frequency error as

$$f_{\text{error}}(k) = E(f_{\text{act}}) - f'_{\text{sw}}. \tag{16}$$

The probability range, $[1/6, 5/6]$, in step 5) is to make sure the proportion of a pulse pattern is no less than $1/6$. With the switching frequency compensation, $E(f_{\text{act}})$ in one calculation

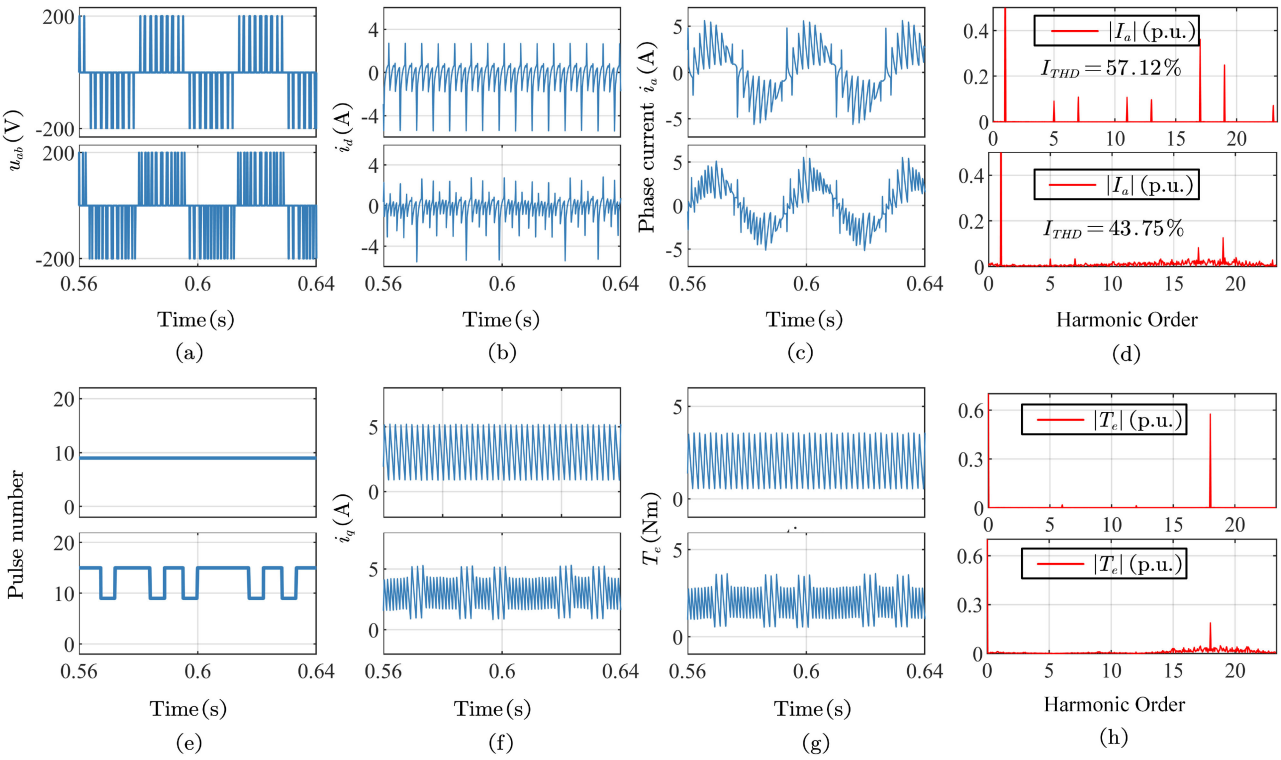

Fig. 10. Simulation results comparison between traditional strategy and the proposed strategy at $I_d = 0$ A, $I_q = 3$ A, and $f_e = 30$ Hz.

may deviate from f_{sw}, but the error is recorded and corrected in further calculation so that the tracking of switching frequency will be accurate.

E. Comparison Between Conventional and Randomized Pulse Pattern Strategy

1) Switching Frequency: Utilization of maximum switching frequency is shown in the curve of f_{sw} versus f_e, and the comparisons of the conventional strategy and the randomized strategy are illustrated in Fig. 11. The allowable switching frequency is assumed 400 Hz. The randomized pulse pattern strategy utilizes the available switching frequency more efficiently so that lower harmonic distortion can be realized compared with the conventional strategy.

2) WTHD0: The WTHD0 curves of the line voltage are depicted in Fig. 12. The modulation index is assumed rising from 0 to 1 in 0–100 Hz. It can be verified that the randomization strategy brings a significant improvement in harmonic distortion due to the higher switching frequency utilization.

The WTHD of the randomized pulse pattern is denoted as WTHD′, which equals the weighted root mean square (rms) of the adopted conventional pulse patterns' WTHD, as

$$\mathrm{WTHD}' = \sqrt{p_1 \mathrm{WTHD}_1^2 + p_2 \mathrm{WTHD}_2^2} \tag{17}$$

where p_1 and p_2 are the proportions of the conventional pulse patterns and WTHD_1 and WTHD_2 are their WTHD, respectively. Following are the detailed deduction.

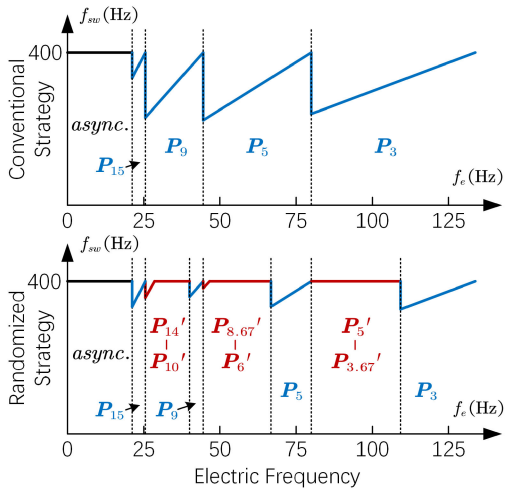

Fig. 11. Switching frequency comparison between the conventional pulse pattern strategy and the randomized pulse pattern strategy.

The relationship of the line voltage's WTHD is similar with relationship of THD of currents when the motor is considered as symmetrical inductive load. However, the latter would be more clear and easy to understand, and is used to illustrate in the following paragraphs.

The harmonic current can be expressed by (18), where $i^1(\tau)$ is the fundamental current, $i(\tau)$ is the actual current, and t_p is

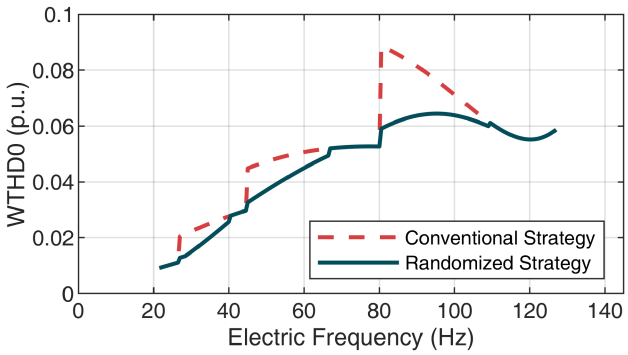

Fig. 12. Harmonic performance of the conventional pulse pattern strategy and the randomized pulse pattern strategy.

the total time

$$i_{\text{rms}}^{\text{h}} = \sqrt{\frac{1}{t_p}\int_{t_0}^{t_0+t_p} \left[i\left(\tau\right) - i^1\left(\tau\right)\right]^2 \mathrm{d}\tau}. \tag{18}$$

There are six pulse pattern units in a fundamental period. We categorize the harmonic current into six parts according to pulse pattern units. Each part of harmonic current is named as current unit. Which results from the corresponding pulse pattern unit. The harmonic current is shown in

$$i_{\text{rms}}^{\text{h}} = \sqrt{\frac{1}{6}\sum_{i=1}^{6}\frac{6}{t_p}\int_{t_0+(i-1)t_p/6}^{t_0+it_p/6} \left[i\left(\tau\right) - i^1\left(\tau\right)\right]^2 \mathrm{d}\tau}. \tag{19}$$

Supposing there are m fundamental periods, and the randomized strategy is applied. The current units from pulse pattern $\boldsymbol{P}_x$ is denoted as i_x and the current units from pulse pattern $\boldsymbol{P}_y$ is represented by i_y as shown in

$$i_{\text{rms}}^{\text{h}} = \sqrt{\frac{1}{m}\sum_{k=0}^{m-1}\left[\frac{1}{6}\sum_{i=0}^{5}\frac{6}{t_p}\int_{t_0+kt_p+it_p/6}^{t_0+kt_p+(i+1)t_p/6} \left[i_{x/y}\left(\tau\right) - i^1\left(\tau\right)\right]^2 \mathrm{d}\tau\right]} \tag{20}$$

$$\begin{aligned} i_{\text{rms}}^{\text{h}} &= \sqrt{\frac{1}{mt_p}\left(\int_{t_0}^{t_0+lt_p} \left[i_x\left(\tau\right) - i^1\left(\tau\right)\right]^2 \mathrm{d}\tau + \int_{t_0+lt_p}^{t_0+mt_p} \left[i_y\left(\tau\right) - i^1\left(\tau\right)\right]^2 \mathrm{d}\tau\right)} \\ &\approx \sqrt{\frac{1}{m}\left(l{i_{x,\text{rms}}^{\text{h}}}^2 + (m-l)\,{i_{y,\text{rms}}^{\text{h}}}^2\right)} \\ &= \sqrt{P_x{i_{x,\text{rms}}^{\text{h}}}^2 + P_y{i_{y,\text{rms}}^{\text{h}}}^2}). \end{aligned} \tag{21}$$

Assuming that fundamental periods m is large enough, it exists 6m current units in all. Among them, $6l$ current units result from pulse pattern $\boldsymbol{P}_x$, and $6(m-l)$ current units result from $\boldsymbol{P}_y$. Due to the randomized strategy, the pulse pattern units of $\boldsymbol{P}_x$ and $\boldsymbol{P}_y$ dispersed equally in six sectors If the current transit smoothly in the pulse pattern unit combination instant, all the 6m current units can be divided into two parts according to their corresponding pulse patterns as shown in (21).

Although the forgoing deduction are conducted in time domain, The conclusion in (21) is also valid for current harmonics at any specific order because the current consistency is kept in pulse pattern units combination instants. Besides, the fundamental current maintained constant after the randomization strategy. The total harmonic current equal to the weighted average of the THD of current resulted from $\boldsymbol{P}_x$ and $\boldsymbol{P}_y$. So is the WTHD relationship of the line voltage.

3) Symmetry Conditions: In traditional synchronized SVPWM, all the pulse patterns are implemented according to symmetry conditions (HWS, QWS, TPS). The pulse sequences meets the periodicity of the fundamental frequency. When applying randomized pulse pattern strategy, the pulse sequences of line voltage are composed of pulse sequences units that come from different pulse patterns. So the line voltage in consecutive line cycles would not be identical. The proposed randomized pulse pattern strategy is achieved according to the probability theory, so the spectrum analysis should be conducted in many line cycles that are as much as possibly in statistical significance rather than a single line cycle, due to the loss of periodicity. In a couple of line cycles, it is prone to conclude that the three symmetry conditions are not qualified. However, it is inaccurate. As the aforementioned deduction of (17) shows that if the line cycles are as much as possible, the pulse pattern units of the same pulse pattern would disperse equally in six sectors, we could categorize the pulse pattern units into two parts and sort them together, respectively, according to their pulse patterns. It would be amazing to see the three symmetry conditions are kept as usual in the two parts, respectively, and the transition between different pulse patterns take place only once. Therefore, the proposed strategy also keep the symmetry characteristics of the conventional synchronized SVPWM.

IV. Simulations and Experiments

The proposed strategy is verified through simulations and experiments. The experiments are carried out on the test bench shown in Fig. 14. A permanent magnet synchronous machine is used as the test machine, and an induction machine is used as the load machine. The inverter is based on the micro control unit TMS320F28335 and the IGBT module PM75RL1A120. The waveform in the experiment is recorded by a Yokogawa ScopeCorder DL850E. The phase currents and line voltages are directly measured from the machine by probes, and the i_d, i_q, and pulse pattern indicator are output by the controller using D/A converters. The parameters of the machine used in the simulations and experiment are shown in Table VI. The switching frequency of the inverter is limited to 400 Hz in simulations and experiments.

A. Results of Simulations

The simulated steady-state current waveforms of the conventional strategy and the proposed strategy are compared in Fig. 10. In this experiment, a complex-gain current controller is used while the speed is controlled by the load machine. The fundamental frequency is 30 Hz, and the current references are $i_q = 3$ A and $i_d = 0$ A. The Conventional strategy uses pulse pattern $\boldsymbol{P}_9$, and the proposed strategy uses the randomized

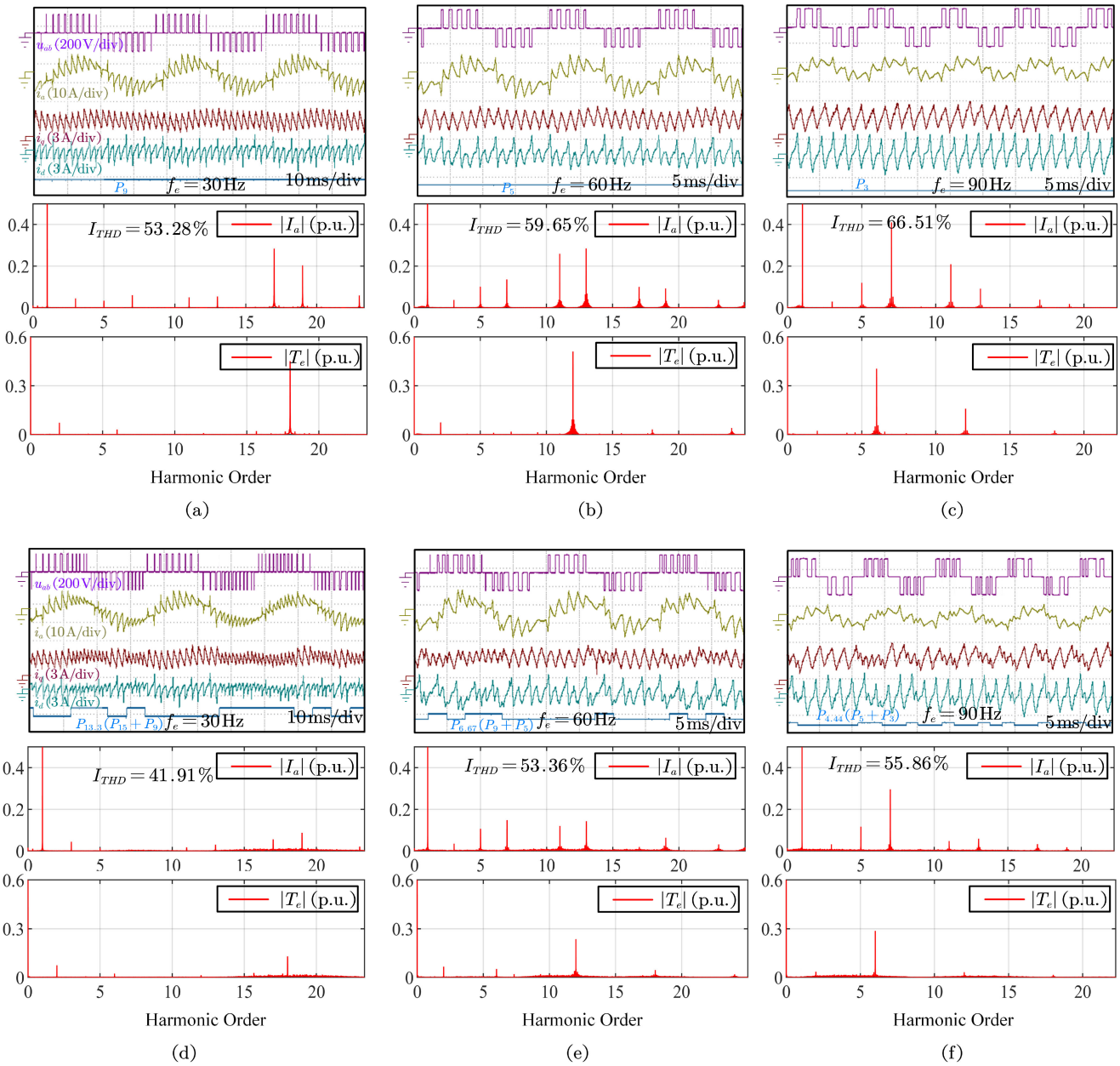

Fig. 13. Experimental comparison between conventional strategy and randomized strategy at $I_d = 0$ A, $I_q = 3$ A. (a)–(c) Waveforms and current spectrum of the conventional strategy. (d)–(f) Waveforms and current spectrum of the randomized strategy.

pulse pattern $\boldsymbol{P}'_{13.33}$. The proposed strategy fully utilizes the available switching frequency so that lower harmonic distortion is realized. Meanwhile, unlike asynchronous SVPWM in low switching frequency applications, the proposed strategy does not generate apparent low-order harmonics. Besides, the current frequency spectrum shows that in the proposed strategy, the centralized harmonic distribution is dispersed, and the peak magnitude of the 17th and the 19th order harmonics are reduced. As Fig. 10(e)–(g) clearly shows the waveform ripples decrease a lot when the pulse pattern unit comes from $\boldsymbol{P}_{15}$. Moreover, the FFT result of torque is presented in (h), which is normalized by the average torque. The primary 18th torque ripple is reduced significantly, and the spectrum is dispersed as the current spectrum.

A frequency-swiping simulation is carried out for comparing the performance between the conventional strategy and the proposed strategy within the full speed range. The results are shown in Fig. 15. The phase current THD is measured every 1 Hz. In the conventional strategy, once the switching frequency exceeds 400 Hz, the modulation switches to a lower-pulse-number patterns. In the randomized strategy, the randomization is enabled in such cases to keep the switching frequency around 400 Hz. A significant reduction in current harmonics can be observed under most operation conditions. In the best case where the machine

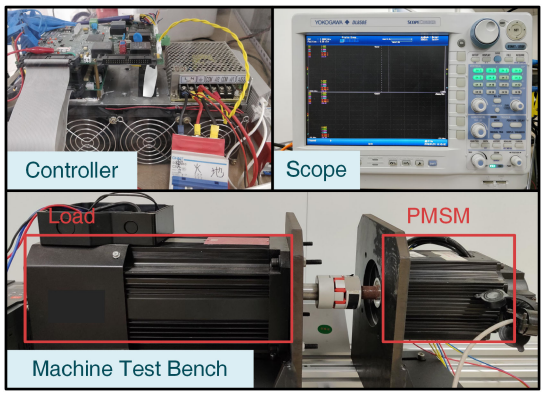

Fig. 14. Photograph of the test bench.

TABLE VI
MACHINE PARAMETERS

Item	Value
DC Voltage	200 V
Rated Power	1.4 kW
Rated Current	8 A
Rated frequency	100 Hz
Number of pole pairs	3
Stator phase resistance	0.75 Ω
Back EMF Constant	0.142 V · s
Stator d-axis Inductance	3.5 mH
Stator q-axis Inductance	9.8 mH

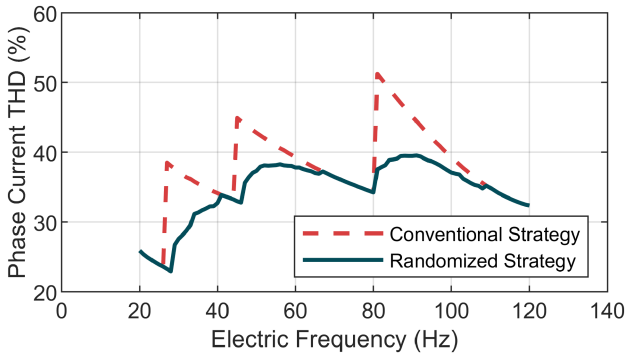

Fig. 15. Harmonic performance of the conventional and the randomized pulse pattern strategy. $i_d = 0$ A, $i_q = 8$ A.

is running at 82 Hz, the THD of phase current reduces from 50.49% to 37.88%.

B. Results of Experiments

The performance of the proposed strategy is also verified on the test bench. As with the simulation, the switching frequency limit is 400 Hz. Fig. 13 shows the comparison of voltage waveforms, current waveforms, and current and torque FFT spectrums between the conventional strategy and the proposed randomized strategy. Thereinto, dq currents and the pulse pattern indicator are output by DA converter, torque are calculated by the sampled dq currents offline and its FFT results are presented. FFT results of torque are normalized by the average

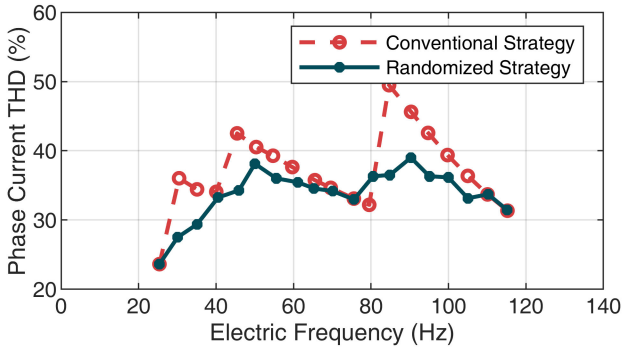

Fig. 16. Comparison of harmonic performance in whole speed range between conventional strategy and randomized strategy. The THD of currents is measured every 5 Hz.

torque. In this experiment, the machine is running under current-closed-loop control with references $i_d = 0$ A and $i_q = 3$ A. In this experiment, some low-order harmonics and side-band harmonics can be observed in the current and torque spectrum of both strategies. The main reason is that the load machine is working as a generator and the power is consumed on a resistor through a chopper circuit. The chopper causes ripples on the bus voltage of the load inverter so that ripples exist on the torque and speed. Besides, the third current harmonic and its corresponding second torque ripple exist in the result, which is resulted from the three phase asymmetry of the test motor. No significant difference can be pointed out between the two strategies on the low-order harmonics and side-band harmonics, which support the explanation that these harmonics are not generated by the randomized strategy. At fundamental frequency of 30, 60, and 90 Hz, the randomized strategy uses pulse pattern $\boldsymbol{P}'_{13.3}$, $\boldsymbol{P}'_{6.67}$, and $\boldsymbol{P}'_{4.44}$, while conventional strategy uses pulse pattern $\boldsymbol{P}_9$, $\boldsymbol{P}_5$, and $\boldsymbol{P}_3$. At these frequencies, the reduction in current harmonic is verified. Besides, the peak magnitude of the 5th, 7th, 11th, and 13th current harmonics are reduced in most of these test cases. the torque FFT results of the proposed strategy shows dispersed spectrum and decrease primary torque ripples significantly compared with that of the conventional strategy.

A frequency-sweeping experiment is accomplished on the test bench. The comparison between the conventional strategy and the proposed strategy is shown in Fig. 16. The value of current THD is measured every 5 Hz. Same as the simulation, the harmonic performance is improved in most of the operating conditions compared with the conventional strategy. The 28.2% reduction in phase current THD can be verified at 85 Hz. However, at 80 Hz, the harmonic performance of the proposed strategy is worser than that of the traditional strategy. Though both strategies has the maximum average switching frequency utilization as shown in Fig. 11, some of the switching actions are used to keep the pulse sequence consistency in the randomized pulse pattern strategy. The switching of conventional strategy is conducted by a hysteresis to avoid frequent switch between pulse patterns, so it has the best harmonic performance with only $\boldsymbol{P}_5$ is applied.

Fig. 17 shows the waveforms of the randomized strategy in the acceleration test. In this test case, a speed-control-loop is enabled in the controller. The effect of randomization can be observed

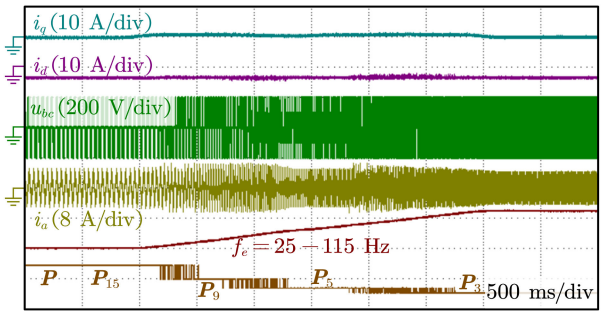

Fig. 17. Experimental results of acceleration with randomized strategy.

in the indicator of pulse pattern $\boldsymbol{P}$ in the waveform, which is switching between adjacent pulse patterns frequently. The randomized strategy works at most operation frequency. With proper controller design and modulation delay compensation, the performance of the current controller and speed controller is not affected by the proposed modulation method.

V. Conclusion

In this article, a randomized pulse pattern strategy of synchronized SVPWM is proposed focusing on improving the performance of the modulation method under low-frequency-ratio conditions. The proposed strategy fills the blank between two adjacent pulse patterns so that the available switching frequency can be fully utilized to reduce harmonic distortion. To realize randomization, the authors analyze the pulse patterns and modify pulse pattern units. Therefore, two units from different pulse patterns can be combined. An algorithm of pulse pattern unit selection is developed to guarantee that the average switching frequency meets the requirement when randomization is employed. Experiments verify the correctness and effectiveness of the proposed strategy.

Currently, the proposed randomized pulse pattern strategy only works on synchronized SVPWM. Meanwhile, other synchronized modulation methods like optimal PWM faces the same problem. It is possible to extend the randomized pulse pattern strategy to more modulation methods, and it will be studied in the future.

References

[1] J. Holtz and N. Oikonomou, "Fast dynamic control of medium voltage drives operating at very low switching frequency-an overview," *IEEE Trans. Ind. Electron.*, vol. 55, no. 3, pp. 1005–1013, Mar. 2008.

[2] J. Holtz and N. Oikonomou, "Synchronous optimal pulsewidth modulation and stator flux trajectory control for medium-voltage drives," *IEEE Trans. Industry Appl.*, vol. 43, no. 2, pp. 600–608, Mar. 2007.

[3] C.-Y. Huang, C.-P. Wei, J.-T. Yu, and Y.-J. Hu, " Torque and current control of induction motor drives for inverter switching frequency reduction," *IEEE Trans. Ind. Electron.*, vol. 52, no. 5, pp. 1364–1371, Oct. 2005.

[4] Z. Peroutka, T. Glasberger, and M. Janda, "Main problems and proposed solutions to induction machine drive control of multisystem locomotive," in *Proc. IEEE Energy Convers. Congr. Exposition.*, Sep. 2009, pp. 430–437.

[5] B. Wu, "High-Power Semiconductor Devices," in *High-Power Converters and Ac Drives*. New York, NY, USA: Wiley, 2006, pp. 17–33.

[6] S. Dieckerhoff, S. Bernet, and D. Krug, " Power loss-oriented evaluation of high voltage IGBTs and multilevel converters in transformerless traction applications," *IEEE Trans. Power Electron.*, vol. 20, no. 6, pp. 1328–1336, Nov. 2005.

[7] G. Narayanan and V. T. Ranganathan, "Synchronised PWM strategies based on space vector approach. I. Principles of waveform generation," *IEE Proc. Electric Power Appl.*, vol. 146, no. 3, pp. 267–275, May 1999.

[8] W. Chen, H. Sun, X. Gu, and C. Xia, "Synchronized space-vector PWM for three-level VSI with lower harmonic distortion and switching frequency," *IEEE Trans. Power Electron.*, vol. 31, no. 9, pp. 6428–6441, Sep. 2016.

[9] M. S. KP, J. Peter, and R. Ramchand, "Space vector based synchronized PWM strategies for field oriented control of VSI fed induction motor," in *Proc. IEEE Int. Conf. Power Electron., Drives Energy Syst.*, Dec. 2016, pp. 1–5.

[10] D. Czarkowski, D. Chudnovsky, and I. Selesnick, "Solving the optimal PWM problem for single-phase inverters," *IEEE Trans. Circuits Syst. I, Fundam. Theory Appl.*, vol. 49, no. 4, pp. 465–475, Apr. 2002.

[11] G. S. Buja and G. B. Indri, "Optimal pulsewidth modulation for feeding AC motors," *IEEE Trans. Industry Appl.*, vol. IA-13, no. 1, pp. 38–44, Jan. 1977.

[12] A. K. Rathore, J. Holtz, and T. Boller, "Synchronous optimal pulsewidth modulation for low-switching-frequency control of medium-voltage multilevel inverters," *IEEE Trans. Ind. Electron.*, vol. 57, no. 7, pp. 2374–2381, Jul. 2010.

[13] J. R. Wells, B. M. Nee, P. L. Chapman, and P. T. Krein, "Selective harmonic control: A general problem formulation and selected solutions," *IEEE Trans. Power Electron.*, vol. 20, no. 6, pp. 1337–1345, Nov. 2005.

[14] Y. Zhang, Y. W. Li, N. R. Zargari, and Z. Cheng, "Improved selective harmonics elimination scheme with online harmonic Compensation for High-Power PWM converters," *IEEE Trans. Power Electron.*, vol. 30, no. 7, pp. 3508–3517, Jul. 2015.

[15] G. Narayanan and V. T. Ranganathan, "Synchronised PWM strategies based on space vector approach. Part 2: Performance assessment and application to V/f drives," *IEE Proc. Electric Power Appl.*, vol. 146, no. 3, pp. 276–281, May 1999.

[16] C. Wang, K. Wang, and X. You, "Research on synchronized SVPWM strategies under low switching frequency for Six-Phase VSI-Fed asymmetrical dual stator induction machine," *IEEE Trans. Ind. Electron.*, vol. 63, no. 11, pp. 6767–6776, Nov. 2016.

[17] L. Diao, J. Tang, P. C. Loh, S. Yin, L. Wang, and Z. Liu, "An efficient DSP–FPGA-Based implementation of hybrid PWM for electric rail traction induction motor control," *IEEE Trans. Power Electron.*, vol. 33, no. 4, pp. 3276–3288, Apr. 2018.

[18] H. Yang, Y. Zhang, G. Yuan, P. D. Walker, and N. Zhang, "Hybrid synchronized PWM schemes for closed loop current control of high power motor drives," *IEEE Trans. Ind. Electron.*, vol. 64, pp. 6920–6929, no. 9, Sep. 2017.

[19] G. Narayanan and V. T. Ranganathan, "Extension of operation of space vector PWM strategies with low switching frequencies using different overmodulation algorithms," *IEEE Trans. Power Electron.*, vol. 17, no. 5, pp. 788–798, Sep. 2002.

[20] A. R. Beig, "Synchronized SVPWM algorithm for the overmodulation region of a Low switching frequency medium-voltage three-level VSI," *IEEE Trans. Ind. Electron.*, vol. 59, no. 12, pp. 4545–4554, Dec. 2012.

[21] R. S. Kanchan, K. Gopakumar, and R. Kennel, "Synchronised carrier-based SVPWM signal generation scheme for the entire modulation range extending up to six-step mode using the sampled amplitudes of reference phase voltages," *IET Electric Power Appl.*, vol. 1, no. 3, pp. 407–415, May 2007.

[22] L. Xiao, J. Li, Y. Xiong, J. Chen, and H. Gao, "Strategy and implementation of harmonic-reduced synchronized svpwm for high-power traction machine drives," *IEEE Trans. Power Electron.*, vol. 35, no. 11, pp. 12 457–12 471, Nov. 2020.

[23] Y.-S. Lai, Y.-T. Chang, and B.-Y. Chen, "Novel random-switching PWM technique With constant sampling frequency and constant inductor average current for digitally controlled converter," *IEEE Trans. Ind. Electron.*, vol. 60, no. 8, pp. 3126–3135, Aug. 2013.

[24] L. Mathe, F. Lungeanu, D. Sera, P. O. Rasmussen, and J. K. Pedersen, "Spread spectrum modulation by using asymmetric-carrier random PWM," *IEEE Trans. Ind. Electron.*, vol. 59, no. 10, pp. 3710–3718, Oct. 2012.

[25] S. E. Schulz and D. L. Kowalewski, "Implementation of variable-delay random PWM for automotive applications," *IEEE Trans. Veh. Technol.*, vol. 56, no. 3, pp. 1427–1433, May 2007.

[26] G. Covic and J. Boys, "Noise quieting with random PWM AC drives," *IEE Proc. Elect. Power Appl.*, vol. 145, no. 1, pp. 1–10, Jan. 1998.

[27] T. Habetler and D. Divan, "Acoustic noise reduction in sinusoidal PWM drives using a randomly modulated carrier," *IEEE Trans. Power Electron.*, vol. 6, no. 3, pp. 356–363, Jul. 1991.